

Model-free Rayleigh weight from x-ray Thomson scattering measurements

T. Dornheim,^{1,2,*} H. M. Bellenbaum,^{1,2,3,4} M. Bethkenhagen,⁵ S. B. Hansen,⁶ M. P. Böhme,^{4,1,2}
 T. Döppner,⁴ L. B. Fletcher,⁷ Th. Gawne,^{1,2} D. O. Gericke,⁸ S. Hamel,⁴ D. Kraus,^{3,2} M. J. MacDonald,⁴
 Zh. A. Moldabekov,^{1,2} Th. R. Preston,⁹ R. Redmer,³ M. Schörner,³ S. Schwalbe,^{1,2} P. Tolia,¹⁰ and J. Vorberger²

¹Center for Advanced Systems Understanding (CASUS), D-02826 Görlitz, Germany

²Helmholtz-Zentrum Dresden-Rossendorf (HZDR), D-01328 Dresden, Germany

³Institut für Physik, Universität Rostock, D-18051 Rostock, Germany

⁴Lawrence Livermore National Laboratory (LLNL), California 94550 Livermore, USA

⁵LULI, CNRS, CEA, Sorbonne Université, École Polytechnique – Institut Polytechnique de Paris, 91128 Palaiseau, France

⁶Sandia National Laboratories, Albuquerque, NM 87185, USA

⁷SLAC National Accelerator Laboratory, Menlo Park California 94309, USA

⁸Centre for Fusion, Space and Astrophysics, University of Warwick, Coventry CV4 7AL, UK

⁹European XFEL, D-22869 Schenefeld, Germany

¹⁰Space and Plasma Physics, Royal Institute of Technology (KTH), Stockholm, SE-100 44, Sweden

X-ray Thomson scattering (XRTS) has emerged as a powerful tool for the diagnostics of matter under extreme conditions. In principle, it gives one access to important system parameters such as the temperature, density, and ionization state, but the interpretation of the measured XRTS intensity usually relies on theoretical models and approximations. In this work, we show that it is possible to extract the Rayleigh weight—a key property that describes the electronic localization around the ions—directly from the experimental data without the need for any model calculations or simulations. As a practical application, we consider an experimental measurement of strongly compressed Be at the National Ignition Facility (NIF) [Döppner *et al.*, *Nature* **618**, 270-275 (2023)]. In addition to being interesting in their own right, our results will open up new avenues for diagnostics from *ab initio* simulations, help to further constrain existing chemical models, and constitute a rigorous benchmark for theory and simulations.

The x-ray Thomson scattering (XRTS) method [1, 2] constitutes a powerful experimental technique, which is capable of giving microscopic insights into a probed sample. A particularly important use case for XRTS is the diagnostics of experiments with matter under extreme densities, temperatures and pressures [3]. Such *warm dense matter* (WDM) [4, 5] naturally occurs in various astrophysical objects such as giant planet interiors [6–8], brown dwarfs [9] and the outer crust of neutron stars [10]. Moreover, WDM plays an important role in a variety of technological applications such as inertial confinement fusion (ICF) [11], where the fuel capsule has to traverse the WDM regime in a controlled way to reach ignition [12]. The recent breakthrough at the National Ignition Facility (NIF) to reach ignition [13] has further substantiated the importance of accurately diagnosing WDM states. In the laboratory, these extreme states can be realized using a variety of experimental techniques [3], and XRTS is often used to infer a-priori unknown system parameters such as the mass density ρ , temperature T , and ionization state Z ; see, e.g., Ref. [14]. These properties can then be used for physical considerations, to inform equation-of-state tables [15–17], and to benchmark integrated multi-scale simulations such as radiation hydrodynamics [18].

In practice, the measured XRTS intensity can be accurately expressed as [19]

$$I(\mathbf{q}, E) = S_{ee}(\mathbf{q}, E) \otimes R(E), \quad (1)$$

where $S_{ee}(\mathbf{q}, E)$ denotes the electronic dynamic structure factor (DSF) that describes the probed system, and $R(E)$ the combined source-and-instrument function (SIF) that takes into account the shape of the x-ray source and effects of the detector [19]. We note that a deconvolution solving Eq. (1) for $S_{ee}(\mathbf{q}, E)$ constitutes a major challenge considering the uncertainties of the SIF and the experimental error bars [20, 21]. Therefore, the usual way to interpret the measured XRTS intensity has been to construct a forward model for $S_{ee}(\mathbf{q}, E)$, convolve it with $R(E)$, and then fit the resulting trial intensity to the LHS of Eq. (1) where the unknown system properties are treated as free parameters. Naturally, the thus inferred information depends on the employed forward model for $S_{ee}(\mathbf{q}, E)$. These are usually based on a number of assumptions such as the possibility to distinguish between *bound* and *free* electrons as proposed within the popular Chihara approach [1, 20–25].

Very recently, it has been proposed to instead consider the two-sided Laplace transform of the DSF [5, 28, 29],

$$F_{ee}(\mathbf{q}, \tau) = \mathcal{L}[S_{ee}(\mathbf{q}, E)] = \int_{-\infty}^{\infty} dE S_{ee}(\mathbf{q}, E) e^{-\tau E}, \quad (2)$$

which is directly related to the imaginary-time density-density correlation function (ITCF) $F_{ee}(\mathbf{q}, \tau)$. The latter naturally emerges in Feynman’s path-integral picture of statistical mechanics [30] and, from a physical perspective, contains the same information as $S_{ee}(\mathbf{q}, E)$, although in an unfamiliar representation [31, 32]. It corresponds to the usual intermediate scattering function $F(\mathbf{q}, t) = \langle \hat{n}(\mathbf{q}, t) \hat{n}(-\mathbf{q}, 0) \rangle$ with an imaginary argument

* t.dornheim@hzdr.de

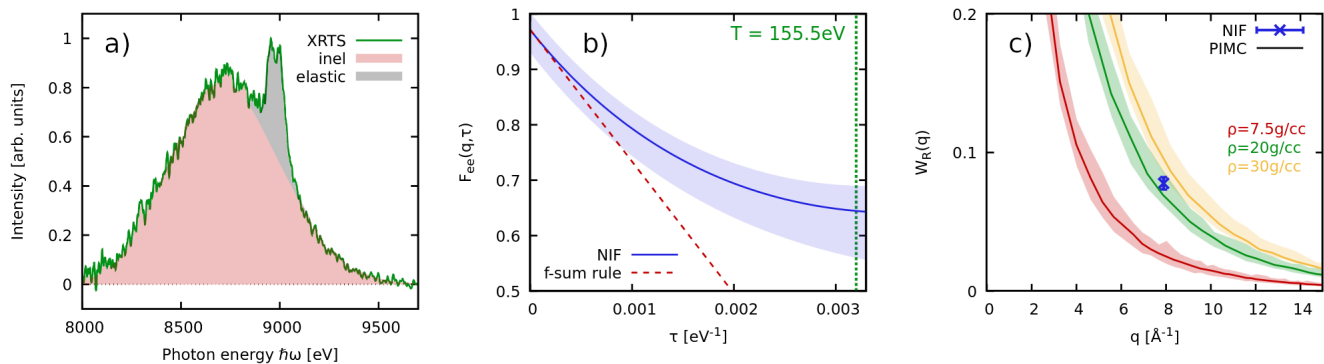


FIG. 1. Left: XRTS measurement on strongly compressed Be at the NIF [24] (green) and its decomposition into elastic (grey) and inelastic (red) contributions. Center: Determination of the normalization $S_{ee}(\mathbf{q}) = F_{ee}(\mathbf{q}, 0)$ from the f-sum rule [26], cf. Eq. (7). Right: Wavenumber dependence of the Rayleigh weight $W_R(\mathbf{q})$, comparing the experimental data point [Eq. (6)] with *ab initio* PIMC simulations [27]; the solid lines have been obtained for $T = 155.5$ eV and the shaded areas correspond to the uncertainty range of ± 15 eV.

$t = -i\hbar\tau$ with $\tau \in [0, \beta]$ and $\beta = 1/k_B T$ the inverse temperature. A key advantage of working in the Laplace domain is given by the convolution theorem

$$\mathcal{L}[S_{ee}(\mathbf{q}, E)] = \frac{\mathcal{L}[S_{ee}(\mathbf{q}, E) \otimes R(E)]}{\mathcal{L}[R(E)]}, \quad (3)$$

which is remarkably stable with respect to experimental noise [26, 29]. Eq. (3) thus gives one direct access to $F_{ee}(\mathbf{q}, \tau)$ from the experimental observation. As a first application, Dornheim *et al.* [28] have suggested to consider the imaginary-time version of the detailed balance relation $F_{ee}(\mathbf{q}, \tau) = F_{ee}(\mathbf{q}, \beta - \tau)$, which gives one model-free access to the temperature of arbitrarily complex systems [25, 28, 29, 33]. A second practical application of the ITCF in the context of XRTS diagnostics is given by the f-sum rule, which relates the first τ -derivative of $F_{ee}(\mathbf{q}, \tau)$ to the momentum transfer $q = |\mathbf{q}|$ that follows from the scattering angle θ [26, 34]. In this way, one can infer the normalization of the measured intensity, which is given by the electronic static structure factor $S_{ee}(\mathbf{q})$ —the Fourier transform of the electron–electron pair correlation function $g_{ee}(\mathbf{r})$. Finally, we mention the recent idea by Vorberger *et al.* [35], who have proposed to utilize Eq. (3) to quantify the degree of electronic non-equilibrium in the probed system.

In the present work, we extend these efforts towards a model-free diagnostics of XRTS measurements by extracting the Rayleigh weight $W_R(\mathbf{q}) = S_{eI}^2(\mathbf{q})/S_{II}(\mathbf{q})$ [where $S_{eI}(\mathbf{q})$ and $S_{II}(\mathbf{q})$ are the electron–ion and ion–ion static structure factor], which describes the degree of electronic localization around the ions [36, 37], directly from the experimental observation. Our idea is based on a combination of the f-sum rule with the ratio of elastic to inelastic scattering $r(\mathbf{q})$, cf. Eq. (5) below. Therefore, it is generally available and even extends to non-equilibrium situations. As a practical example, we consider an XRTS measurement on strongly compressed Be that has been carried out at the NIF [24].

The proposed direct inference of $W_R(\mathbf{q})$ helps to further constrain forward models for the interpretation of XRTS measurements, which is very important in its own right. In addition, we expect $W_R(\mathbf{q})$ to be a valuable diagnostic tool. For example, one might first infer the temperature T from a given XRTS signal using the model-free ITCF method [28] and then carry out a set of *ab initio* calculations for $W_R(\mathbf{q})$ over a reasonable interval of densities ρ ; here, we use highly accurate path integral Monte Carlo (PIMC) simulations using the set-up described in Ref. [27] and density functional theory molecular dynamics (DFT-MD) simulations by Bethkenhagen *et al.* [38]. We find excellent agreement between both methods, whereas computationally less involved average-atom models [39] and Chihara fits deviate. This is of direct practical consequence for the interpretation of the experimental signal and suggests a significantly lower density of $\rho = (22 \pm 2)$ g/cm³ (see also Ref. [27]) compared to the Chihara based estimate of $\rho = (34 \pm 4)$ g/cm³ by Döppner *et al.* [24].

From a methodological perspective, we note that $W_R(\mathbf{q})$ constitutes a perfect observable for DFT-MD, as it only involves the static single-electron density distribution $n_e(\mathbf{r})$ [and the ion density distribution and correlation function, which are both easily accessible within MD]. This is in contrast to time-dependent DFT (TD-DFT) calculations that, in practice, contain additional approximations such as the unknown dynamic exchange–correlation kernel in the case of linear-response TD-DFT [33, 40–42]. Finally, we mention the possibility to use experimental results for $W_R(\mathbf{q})$ as a rigorous benchmark for simulations and theoretical models in situations where the density and temperature are already being known by other means.

Idea. In general, we can split the DSF into a quasi-elastic contribution $S_{el}(\mathbf{q}, E)$ that is due to the electronic localization around the ions described by the Rayleigh

weight, and the inelastic part $S_{\text{inel}}(\mathbf{q}, E)$ [cf. Fig. 1a)],

$$S_{ee}(\mathbf{q}, E) = \underbrace{W_R(\mathbf{q})\delta(E)}_{S_{\text{el}}(\mathbf{q}, E)} + S_{\text{inel}}(\mathbf{q}, E). \quad (4)$$

Here, the quasi-elastic nature of the first part is due to the substantially longer ionic time-scales. In practice, treating $S_{\text{el}}(\mathbf{q}, E)$ as a delta distribution is appropriate if the SIF $R(E)$ is significantly broader than the actual ion feature. This is usually the case except for dedicated experiments that aim to resolve ionic energy scales on purpose [43]. Within the chemical picture that assumes a decomposition into effectively *bound* and *free* electrons [1, 23, 24, 44], the inelastic part $S_{\text{inel}}(\mathbf{q}, E)$ consists of both bound-free transitions (and their reverse process [25]) and free-free transitions. The Rayleigh weight thus constitutes an indispensable ingredient to Chihara models [22, 44] that are widely used for the interpretation of XRTS experiments with WDM [1, 23–25]. However, it is important to note that we do not have to make such an approximate distinction between bound and free electrons in the present work.

Let us next consider the ratio of the elastic and inelastic contributions

$$r(\mathbf{q}) = \frac{\int_{-\infty}^{\infty} d\omega S_{\text{el}}(\mathbf{q}, \omega)}{\int_{-\infty}^{\infty} d\omega S_{\text{inel}}(\mathbf{q}, \omega)} = \frac{W_R(\mathbf{q})}{S_{ee}(\mathbf{q}) - W_R(\mathbf{q})}, \quad (5)$$

that constitutes a standard observable in XRTS experiments [24], see, e.g., Fig. 1a). Here $S_{ee}(\mathbf{q}) = F_{ee}(\mathbf{q}, 0)$ denotes the aforementioned electronic static structure factor that we can also directly extract from the XRTS signal using the f-sum rule applied in the imaginary-time domain as it has been explained in detail in the recent Ref. [26], see also Eq. (7) below. Solving Eq. (5) for the Rayleigh weight then gives

$$W_R(\mathbf{q}) = \frac{S_{ee}(\mathbf{q})}{1 + r^{-1}(\mathbf{q})}. \quad (6)$$

Results. In Fig. 1, we apply our new idea to an XRTS data set that has been recently obtained at the NIF by Döppner *et al.* [24]. Panel a) shows the full XRTS intensity [solid green, cf. Eq. (1)], which can easily be decomposed into its elastic (grey) and inelastic (red) contribution if the SIF $R(E)$ is known; this is indeed the case for the backlighter x-ray source utilized at the NIF [45]. The second ingredient to Eq. (6) is given by the electronic static structure factor $S_{ee}(\mathbf{q})$, which we obtain from the Laplace transform of the XRTS signal via the f-sum rule. This procedure is illustrated in Fig. 1b), where we show the deconvolved $F_{ee}(\mathbf{q}, \tau)$ as a function of τ . In the imaginary-time domain, the f-sum rule is given by [26, 31, 34]

$$\left. \frac{\partial}{\partial \tau} F_{ee}(\mathbf{q}, \tau) \right|_{\tau=0} = -\frac{\hbar^2 \mathbf{q}^2}{2m_e}; \quad (7)$$

matching Eq. (7) [dashed red line] with the LHS. of Eq. (3) [solid blue line] around $\tau = 0$ then determines

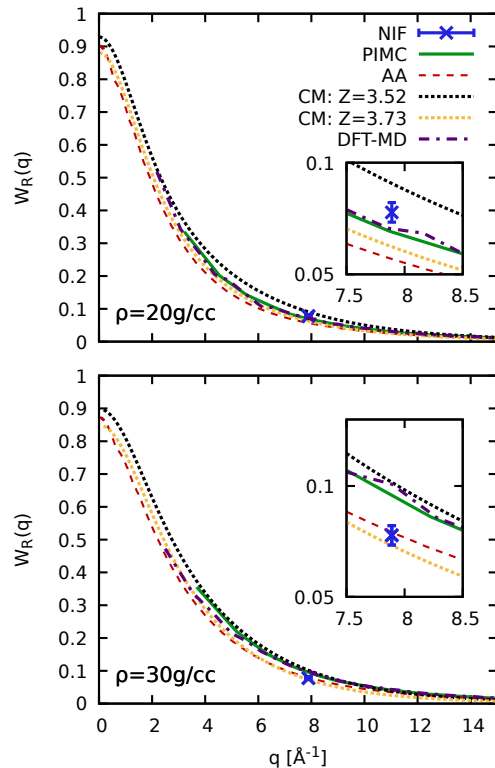


FIG. 2. Comparison of simulation results for the Rayleigh weight at $\rho = 20$ g/cc [top] and $\rho = 30$ g/cc [bottom]. Blue cross: experiment [24]; solid green: PIMC; dashed red: average atom model; black and yellow dotted: chemical model with ionization states of $Z = 3.52$ and $Z = 3.73$; dash-dotted purple: DFT-MD [38]. PIMC and CM have been computed for $T = 155.5$ eV, DFT-MD and AA for $T = 150$ eV.

the a-priori unknown normalization constant and, in turn, $S_{ee}(\mathbf{q}) = F_{ee}(\mathbf{q}, 0)$. Inserting $r(\mathbf{q})$ and $S_{ee}(\mathbf{q})$ into Eq. (6) gives our final, model-free estimate of the Rayleigh weight, which is shown as the blue cross in Fig. 1c) at the corresponding experimental wavenumber of $q = 7.89 \text{ \AA}^{-1}$. The red, green and yellow solid curves in the panel show highly accurate *ab initio* PIMC results that have been obtained for $N_{\text{Be}} = 10$ Be atoms using the set-up described in the recent Refs. [27, 46] at the temperature of $T = 155.5$ eV that has been inferred from the symmetry of the ITCF; see the appendix of Ref. [27] for additional details. In addition, the associated colored areas correspond to PIMC simulations for $T = (155.5 \pm 15)$ eV and indicate the uncertainty in the Rayleigh weight at a given density due to the uncertainty in the inferred temperature. Fig. 1 thus indicates a mass density of $\rho \approx 20$ g/cm³, whereas the nominal result of $\rho = (34 \pm 4)$ g/cm³ reported in the original Ref. [24] is ruled out.

To get further insights into the sensitivity of the interpretation of a given XRTS measurement to the employed model or simulation technique, we compare a number of independent methods in Fig. 2, where the top and bottom

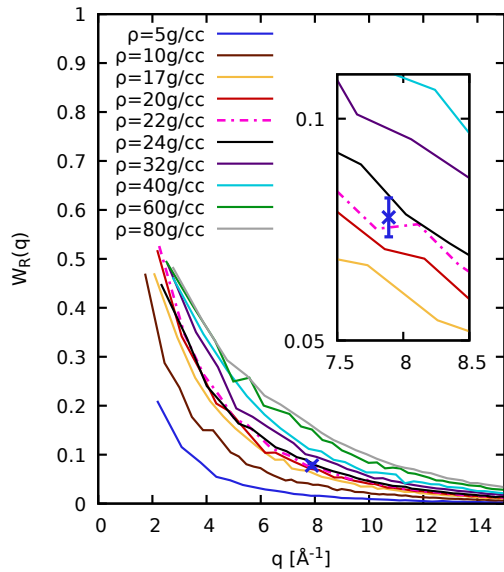


FIG. 3. Curves: DFT-MD results for $W_R(\mathbf{q})$ at $T = 150$ eV for different mass densities ρ . The experimental measurement (blue cross) at the NIF [24] is associated with a density of $\rho = 22 \pm 2$ g/cc [dash-dotted pink], see also the inset showing a magnified segment.

panels correspond to $\rho = 20$ g/cm³ and $\rho = 30$ g/cm³, respectively. For both cases, we find very good agreement between PIMC (solid green) and DFT-MD simulations by Bethkenhagen *et al.* [38] (dash-dotted purple). The computationally cheaper average-atom model [39] (dashed red) is in qualitative, though not quantitative agreement with the *ab initio* data sets. Instead, it agrees with the experimental data point for $\rho = 30$ g/cm³. This clearly highlights the sensitivity of equation-of-state measurements to the proper treatment of electronic correlations and other many-body effects in the analysis of the experimental observation. Finally, we include two chemical models for the hypothetical ionization degrees of $Z = 3.52$ (dotted black) and $Z = 3.73$ (dotted yellow) for both densities, see the Supplemental Material for additional details [47]. Evidently, the inferred density strongly depends on the inferred ionization state, making the invocation of additional constraints desirable. In Ref. [24], Döppner *et al.* have used the Saha equation in combination with a semi-empirical form factor lowering model for this purpose, leading to the nominal parameters of $\rho = (34 \pm 4)$ g/cm³ and $Z = 3.4 \pm 0.1$. A systematic investigation of the origin of this discrepancy between their chemical model and the *ab initio* data sets from PIMC and DFT-MD is beyond the scope of the present work and will be pursued in a dedicated future study.

Let us conclude with a systematic analysis of the dependence of $W_R(\mathbf{q})$ on the density that is shown in Fig. 3 based on extensive DFT-MD results for $\rho = (5 - 80)$ g/cm³ at $T = 150$ eV. The main trend is given

by the systematic increase of the Rayleigh weight with ρ , which is to a large degree due to the different length scales in the system; the effect almost vanishes when one adjusts the x -axis by the Fermi wavenumber $q_F \sim 1/\rho^{1/3}$. The inset shows a magnified segment around the experimental data point, with the latter being located between the DFT-MD results for $\rho = 20$ g/cm³ (red) and $\rho = 24$ g/cm³ (black); this leads to our final estimate for the density of $\rho = (22 \pm 2)$ g/cm³ [dash-dotted pink].

Summary and Discussion. We have presented a new approach for the model-free extraction of the Rayleigh weight $W_R(\mathbf{q})$ from XRTS measurements. Most importantly, $W_R(\mathbf{q})$ constitutes an important measure for the electronic localization around the ions, which is interesting in its own right. In addition, $W_R(\mathbf{q})$ is of direct practical value for XRTS diagnostics, as we have demonstrated in detail on a recent experiment with strongly compressed beryllium at the NIF [24]. In particular, we propose to first infer the temperature T from the model-free ITCF thermometry approach [28, 29], and to subsequently match the experimental result for $W_R(\mathbf{q})$ with simulation results over a reasonable range of densities. We note that $W_R(\mathbf{q})$ is a particularly suitable observable for DFT-MD simulations, as it does not involve any dynamic information such as the a-priori unknown dynamic exchange-correlation kernel. We find excellent agreement between DFT-MD and PIMC reference data; this is encouraging since direct PIMC simulations are still limited to low- Z materials at moderate to high temperatures [48, 49], whereas DFT-MD is more broadly applicable. An additional advantage of $W_R(\mathbf{q})$ over alternative observables such as the ratio of elastic to inelastic scattering $r(\mathbf{q})$ is that the former does not require any explicit information about the electronic static structure factor $S_{ee}(\mathbf{q})$, which is notoriously difficult for DFT-based methodologies.

In practice, we infer a mass density of $\rho = (22 \pm 2)$ g/cm³ from the beryllium data set using either PIMC or DFT-MD simulations, which is significantly lower than the nominal value of $\rho = (34 \pm 4)$ g/cm³ that has been reported in the original publication based on a chemical Chihara model. Moreover, we find that the computationally cheaper average-atom model tends to overestimate the density, whereas chemical models generally require additional constraints for parameters such as the ionization degree. Our study thus clearly highlights the importance of an accurate treatment of quantum many-body effects for XRTS based equation-of-state measurements even at relatively high temperatures; the main value of average-atom calculations is their low computational efforts, making them a useful tool to constrain the parameter space for more expensive *ab initio* simulations.

We are convinced that our work opens up new possibilities for the study of warm dense matter and beyond. An important point for future research is given by the sensitivity of the inferred Rayleigh weight to the SIF $R(E)$, which is usually modelled for backlighter set-ups [45], but can be known with high precision at modern XFEL fa-

cilities [19]. Indeed, recent advances in high-resolution XRTS measurements [50] at the European XFEL will likely facilitate the application of the model-free ITCF thermometry technique even at moderate temperatures of $T \sim 1$ eV, which are of relevance for both planetary and material science; the current model-free framework for the extraction of $W_R(\mathbf{q})$ is applicable at any temperature. In combination, these two methods will allow for accurate equation-of-state measurements in previously inaccessible regimes. Finally, we mention the intriguing possibility of performing an XRTS experiment on an isochorically heated sample with an appropriate delay between pump and probe to ensure proper equilibration. Since both T and ρ would be well known in such a scenario, a corresponding measurement of $W_R(\mathbf{q})$ using the present framework would constitute a truly unambiguous reference data set for the rigorous benchmarking of *ab initio* simulations and chemical models alike.

ACKNOWLEDGMENTS

This work was partially supported by the Center for Advanced Systems Understanding (CASUS), financed by Germany’s Federal Ministry of Education and Research (BMBF) and the Saxon state government out of the State budget approved by the Saxon State Parliament. This work has received funding from the European Union’s Just Transition Fund (JTF) within

the project *Röntgenlaser-Optimierung der Laserfusion* (ROLF), contract number 5086999001, co-financed by the Saxon state government out of the State budget approved by the Saxon State Parliament. This work has received funding from the European Research Council (ERC) under the European Union’s Horizon 2022 research and innovation programme (Grant agreement No. 101076233, ”PREXTREME”). This work was partially supported by the German Research Foundation (DFG) within the Research Unit FOR 2440. Views and opinions expressed are however those of the authors only and do not necessarily reflect those of the European Union or the European Research Council Executive Agency. Neither the European Union nor the granting authority can be held responsible for them. Computations were performed on a Bull Cluster at the Center for Information Services and High-Performance Computing (ZIH) at Technische Universität Dresden and at the Norddeutscher Verbund für Hoch- und Höchstleistungsrechnen (HLRN) under grants mvp00018 and mvp00024. SH was supported by Sandia National Laboratories, a multi-mission laboratory managed and operated by National Technology and Engineering Solutions of Sandia, LLC, a wholly owned subsidiary of Honeywell International, Inc., for DOE’s National Nuclear Security Administration under contract DE-NA0003525. This paper describes objective technical results and analysis. Any subjective views or opinions that might be expressed in the paper do not necessarily represent the views of the U.S. Department of Energy or the United States Government.

-
- [1] S. H. Glenzer and R. Redmer, “X-ray thomson scattering in high energy density plasmas,” *Rev. Mod. Phys.* **81**, 1625 (2009).
- [2] J. Sheffield, D. Froula, S.H. Glenzer, and N.C. Luhmann, *Plasma Scattering of Electromagnetic Radiation: Theory and Measurement Techniques* (Elsevier Science, 2010).
- [3] K. Falk, “Experimental methods for warm dense matter research,” *High Power Laser Sci. Eng* **6**, e59 (2018).
- [4] F. Graziani, M. P. Desjarlais, R. Redmer, and S. B. Trickey, eds., *Frontiers and Challenges in Warm Dense Matter* (Springer, International Publishing, 2014).
- [5] Tobias Dornheim, Zhandos A. Moldabekov, Kushal Ramakrishna, Panagiotis Talias, Andrew D. Baczewski, Dominik Kraus, Thomas R. Preston, David A. Chapman, Maximilian P. Böhme, Tilo Döppner, Frank Graziani, Michael Bonitz, Attila Cangi, and Jan Vorberger, “Electronic density response of warm dense matter,” *Physics of Plasmas* **30**, 032705 (2023).
- [6] Alessandra Benuzzi-Mounaix, Stéphane Mazevet, Alessandra Ravasio, Tommaso Vinci, Adrien Denoed, Michel Koenig, Nourou Amadou, Erik Brambrink, Floriane Festa, Anna Levy, Marion Harmand, Stéphanie Brygoo, Gael Huser, Vanina Recoules, Johan Bouchet, Guillaume Morard, François Guyot, Thibaut de Resseguier, Kohei Myanishi, Norimasa Ozaki, Fabien Dorchies, Jérôme Gaudin, Pierre Marie Leguay, Olivier Peyrusse, Olivier Henry, Didier Raffestin, Sebastien Le Pape, Ray Smith, and Riccardo Musella, “Progress in warm dense matter study with applications to planetology,” *Phys. Scripta* **T161**, 014060 (2014).
- [7] Tristan Guillot *et al.*, “Giant planets from the inside-out,” (2022), [arXiv:2205.04100](https://arxiv.org/abs/2205.04100) [astro-ph.EP].
- [8] R.P. Drake, *High-Energy-Density Physics: Foundation of Inertial Fusion and Experimental Astrophysics*, Graduate Texts in Physics (Springer International Publishing, 2018).
- [9] A. Becker, W. Lorenzen, J. J. Fortney, N. Nettelmann, M. Schöttler, and R. Redmer, “Ab initio equations of state for hydrogen (h-reos.3) and helium (he-reos.3) and their implications for the interior of brown dwarfs,” *Astrophys. J. Suppl. Ser* **215**, 21 (2014).
- [10] E. H. Gudmundsson, C. J. Pethick, and R. I. Epstein, “Structure of neutron star envelopes,” *Astrophys. J.* **272**, 286–300 (1983).
- [11] R. Betti and O. A. Hurricane, “Inertial-confinement fusion with lasers,” *Nature Physics* **12**, 435–448 (2016).
- [12] S. X. Hu, B. Militzer, V. N. Goncharov, and S. Skupsky, “First-principles equation-of-state table of deuterium for inertial confinement fusion applications,” *Phys. Rev. B* **84**, 224109 (2011).
- [13] The Indirect Drive ICF Collaboration, “Achievement of target gain larger than unity in an inertial fusion exper-

- iment,” *Phys. Rev. Lett.* **132**, 065102 (2024).
- [14] Kai-Uwe Plagemann, Hannes R. Rüter, Thomas Bornath, Mohammed Shihab, Michael P. Desjarlais, Carsten Fortmann, Siegfried H. Glenzer, and Ronald Redmer, “Ab initio calculation of the ion feature in x-ray thomson scattering,” *Phys. Rev. E* **92**, 013103 (2015).
- [15] K. Falk, S.P. Regan, J. Vorberger, M.A. Barrios, T.R. Boehly, D.E. Fratanduono, S.H. Glenzer, D.G. Hicks, S.X. Hu, C.D. Murphy, P.B. Radha, S. Rothman, A.P. Jephcoat, J.S. Wark, D.O. Gericke, and G. Gregori, “Self-consistent measurement of the equation of state of liquid deuterium,” *High Energy Density Physics* **8**, 76–80 (2012).
- [16] K. Falk, E. J. Gamboa, G. Kagan, D. S. Montgomery, B. Srinivasan, P. Tzeferacos, and J. F. Benage, “Equation of state measurements of warm dense carbon using laser-driven shock and release technique,” *Phys. Rev. Lett.* **112**, 155003 (2014).
- [17] J.A. Gaffney, S.X. Hu, P. Arnault, A. Becker, L.X. Benedict, T.R. Boehly, P.M. Celliers, D.M. Ceperley, O. Čertík, J. Clérouin, G.W. Collins, L.A. Collins, J.-F. Danel, N. Desbiens, M.W.C. Dharma-wardana, Y.H. Ding, A. Fernandez-Pañella, M.C. Gregor, P.E. Grabowski, S. Hamel, S.B. Hansen, L. Harbour, X.T. He, D.D. Johnson, W. Kang, V.V. Karasiev, L. Kazandjian, M.D. Knudson, T. Ogitsu, C. Pierleoni, R. Piron, R. Redmer, G. Robert, D. Saumon, A. Shamp, T. Sjostrom, A.V. Smirnov, C.E. Starrett, P.A. Sterne, A. Wardlow, H.D. Whitley, B. Wilson, P. Zhang, and E. Zurek, “A review of equation-of-state models for inertial confinement fusion materials,” *High Energy Density Physics* **28**, 7–24 (2018).
- [18] G.C. Pomraning, *The Equations of Radiation Hydrodynamics*, Dover books on physics (Dover Publications, 2005).
- [19] Thomas Gawne, Hannah Bellenbaum, Luke B. Fletcher, Karen Appel, Carsten Baetz, Victorien Bouffetier, Erik Brambrink, Danielle Brown, Attila Cangi, Adrien Descamps, Sebastian Göde, Nicholas J. Hartley, Marie-Luise Herbert, Philipp Hesselbach, Hauke Höppner, Oliver S. Humphries, Zuzana Konôpková, Alejandro Laso, Björn Lindqvist, Julian Lütgert, Michael J. MacDonald, Mikako Makita, Willow Martin, Mikhail Mishchenko, Zhandos A. Moldabekov, Motoaki Nakatsutsumi, Jean-Paul Naedler, Paul Neumayer, Alexander Pelka, Chongbing Qu, Lisa Randolph, Johannes Rips, Toma Toncian, Jan Vorberger, Lennart Wollenweber, Ulf Zastra, Dominik Kraus, Thomas R. Preston, and Tobias Dornheim, “Effects of mosaic crystal instrumentation functions on x-ray thomson scattering diagnostics,” (2024), [arXiv:2406.03301](https://arxiv.org/abs/2406.03301) [physics.plasm-ph].
- [20] A. Höll, Th. Bornath, L. Cao, T. Döppner, S. Düsterer, E. Förster, C. Fortmann, S.H. Glenzer, G. Gregori, T. Laarmann, K.-H. Meiwes-Broer, A. Przystawik, P. Radcliffe, R. Redmer, H. Reinholz, G. Röpke, R. Thiele, J. Tiggesbäumker, S. Toleikis, N.X. Truong, T. Tschentscher, I. Uschmann, and U. Zastra, “Thomson scattering from near-solid density plasmas using soft x-ray free electron lasers,” *High Energy Density Physics* **3**, 120–130 (2007).
- [21] C. Fortmann, T. Bornath, R. Redmer, H. Reinholz, G. Röpke, V. Schwarz, and R. Thiele, “X-ray thomson scattering cross-section in strongly correlated plasmas,” *Laser and Particle Beams* **27**, 311–319 (2009).
- [22] J Chihara, “Difference in x-ray scattering between metallic and non-metallic liquids due to conduction electrons,” *Journal of Physics F: Metal Physics* **17**, 295–304 (1987).
- [23] D. Kraus, B. Bachmann, B. Barbrel, R. W. Falcone, L. B. Fletcher, S. Frydrych, E. J. Gamboa, M. Gauthier, D. O. Gericke, S. H. Glenzer, S. Göde, E. Granados, N. J. Hartley, J. Helfrich, H. J. Lee, B. Nagler, A. Ravasio, W. Schumaker, J. Vorberger, and T. Döppner, “Characterizing the ionization potential depression in dense carbon plasmas with high-precision spectrally resolved x-ray scattering,” *Plasma Phys. Control Fusion* **61**, 014015 (2019).
- [24] T. Döppner, M. Bethkenhagen, D. Kraus, P. Neumayer, D. A. Chapman, B. Bachmann, R. A. Baggott, M. P. Böhme, L. Divol, R. W. Falcone, L. B. Fletcher, O. L. Landen, M. J. MacDonald, A. M. Saunders, M. Schörner, P. A. Sterne, J. Vorberger, B. B. L. Witte, A. Yi, R. Redmer, S. H. Glenzer, and D. O. Gericke, “Observing the onset of pressure-driven k-shell delocalization,” *Nature* **618**, 270–275 (2023).
- [25] Maximilian P. Böhme, Luke B. Fletcher, Tilo Döppner, Dominik Kraus, Andrew D. Baczewski, Thomas R. Preston, Michael J. MacDonald, Frank R. Graziani, Zhandos A. Moldabekov, Jan Vorberger, and Tobias Dornheim, “Evidence of free-bound transitions in warm dense matter and their impact on equation-of-state measurements,” (2023), [arXiv:2306.17653](https://arxiv.org/abs/2306.17653) [physics.plasm-ph].
- [26] T. Dornheim, T. Döppner, A. D. Baczewski, P. Tolias, M. P. Böhme, Zh. A. Moldabekov, Th. Gawne, D. Ranjan, D. A. Chapman, M. J. MacDonald, Th. R. Preston, D. Kraus, and J. Vorberger, “X-ray thomson scattering absolute intensity from the f-sum rule in the imaginary-time domain,” *Scientific Reports* **14**, 14377 (2024).
- [27] Tobias Dornheim, Tilo Döppner, Panagiotis Tolias, Maximilian Böhme, Luke Fletcher, Thomas Gawne, Frank Graziani, Dominik Kraus, Michael MacDonald, Zhandos Moldabekov, Sebastian Schwalbe, Dirk Gericke, and Jan Vorberger, “Unraveling electronic correlations in warm dense quantum plasmas,” (2024), [arXiv:2402.19113](https://arxiv.org/abs/2402.19113) [physics.plasm-ph].
- [28] Tobias Dornheim, Maximilian Böhme, Dominik Kraus, Tilo Döppner, Thomas R. Preston, Zhandos A. Moldabekov, and Jan Vorberger, “Accurate temperature diagnostics for matter under extreme conditions,” *Nature Communications* **13**, 7911 (2022).
- [29] Tobias Dornheim, Maximilian P. Böhme, David A. Chapman, Dominik Kraus, Thomas R. Preston, Zhandos A. Moldabekov, Niclas Schlünzen, Attila Cangi, Tilo Döppner, and Jan Vorberger, “Imaginary-time correlation function thermometry: A new, high-accuracy and model-free temperature analysis technique for x-ray Thomson scattering data,” *Physics of Plasmas* **30**, 042707 (2023).
- [30] H. Kleinert, *Path Integrals in Quantum Mechanics, Statistics, Polymer Physics, and Financial Markets*, EBL-Schweitzer (World Scientific, 2009).
- [31] Tobias Dornheim, Zhandos Moldabekov, Panagiotis Tolias, Maximilian Böhme, and Jan Vorberger, “Physical insights from imaginary-time density–density correlation functions,” *Matter and Radiation at Extremes* **8**, 056601 (2023).
- [32] Tobias Dornheim, Jan Vorberger, Zhandos A. Moldabekov, and Maximilian Böhme, “Analysing the dynamic structure of warm dense matter in the imaginary-time domain: theoretical models and simulations,” *Philo-*

- sophical Transactions of the Royal Society A: Mathematical, Physical and Engineering Sciences **381**, 20220217 (2023).
- [33] Maximilian Schörner, Mandy Bethkenhagen, Tilo Döppner, Dominik Kraus, Luke B. Fletcher, Siegfried H. Glenzer, and Ronald Redmer, “X-ray thomson scattering spectra from density functional theory molecular dynamics simulations based on a modified chihara formula,” *Phys. Rev. E* **107**, 065207 (2023).
- [34] Tobias Dornheim, Damar C. Wicaksono, Juan E. Suarez-Cardona, Panagiotis Toliias, Maximilian P. Böhme, Zhandos A. Moldabekov, Michael Hecht, and Jan Vorberger, “Extraction of the frequency moments of spectral densities from imaginary-time correlation function data,” *Phys. Rev. B* **107**, 155148 (2023).
- [35] Jan Vorberger, Thomas R. Preston, Nikita Medvedev, Maximilian P. Böhme, Zhandos A. Moldabekov, Dominik Kraus, and Tobias Dornheim, “Revealing non-equilibrium and relaxation in laser heated matter,” *Physics Letters A* **499**, 129362 (2024).
- [36] J. Vorberger and D. O. Gericke, “Ab initio approach to model x-ray diffraction in warm dense matter,” *Phys. Rev. E* **91**, 033112 (2015).
- [37] T. Ma, T. Döppner, R. W. Falcone, L. Fletcher, C. Fortmann, D. O. Gericke, O. L. Landen, H. J. Lee, A. Pak, J. Vorberger, K. Wünsch, and S. H. Glenzer, “X-ray scattering measurements of strong ion-ion correlations in shock-compressed aluminum,” *Phys. Rev. Lett.* **110**, 065001 (2013).
- [38] M. Bethkenhagen, M. Schörner, and R. Redmer, “Insights on the electronic structure of high-density beryllium from ab initio simulations,” Submitted for publication.
- [39] P.A. Sterne, S.B. Hansen, B.G. Wilson, and W.A. Isaacs, “Equation of state, occupation probabilities and conductivities in the average atom Purgatorio code,” *High Energy Density Phys.* **3**, 278–282 (2007).
- [40] C. Ullrich, *Time-Dependent Density-Functional Theory: Concepts and Applications*, Oxford Graduate Texts (OUP Oxford, 2012).
- [41] Zhandos Moldabekov, Maximilian Böhme, Jan Vorberger, David Blaschke, and Tobias Dornheim, “Ab initio static exchange–correlation kernel across jacob’s ladder without functional derivatives,” *Journal of Chemical Theory and Computation* **19**, 1286–1299 (2023).
- [42] Zhandos A. Moldabekov, Michele Pavanello, Maximilian P. Böhme, Jan Vorberger, and Tobias Dornheim, “Linear-response time-dependent density functional theory approach to warm dense matter with adiabatic exchange-correlation kernels,” *Phys. Rev. Res.* **5**, 023089 (2023).
- [43] A. Descamps, B. K. Ofori-Okai, K. Appel, V. Cerantola, A. Comley, J. H. Eggert, L. B. Fletcher, D. O. Gericke, S. Göde, O. Humphries, O. Karnbach, A. Lazicki, R. Loetzsch, D. McGonegle, C. A. J. Palmer, C. Plueckthun, T. R. Preston, R. Redmer, D. G. Senesky, C. Strohm, I. Uschmann, T. G. White, L. Wollenweber, G. Monaco, J. S. Wark, J. B. Hastings, U. Zastra, G. Gregori, S. H. Glenzer, and E. E. McBride, “An approach for the measurement of the bulk temperature of single crystal diamond using an x-ray free electron laser,” *Scientific Reports* **10**, 14564 (2020).
- [44] G. Gregori, S. H. Glenzer, W. Rozmus, R. W. Lee, and O. L. Landen, “Theoretical model of x-ray scattering as a dense matter probe,” *Phys. Rev. E* **67**, 026412 (2003).
- [45] M. J. MacDonald, A. M. Saunders, B. Bachmann, M. Bethkenhagen, L. Divol, M. D. Doyle, L. B. Fletcher, S. H. Glenzer, D. Kraus, O. L. Landen, H. J. LeFevre, S. R. Klein, P. Neumayer, R. Redmer, M. Schörner, N. Whiting, R. W. Falcone, and T. Döppner, “Demonstration of a laser-driven, narrow spectral bandwidth x-ray source for collective x-ray scattering experiments,” *Physics of Plasmas* **28**, 032708 (2021).
- [46] Tobias Dornheim, Sebastian Schwalbe, Maximilian Böhme, Zhandos Moldabekov, Jan Vorberger, and Panagiotis Toliias, “Ab initio path integral monte carlo simulations of warm dense two-component systems without fixed nodes: structural properties,” *J. Chem. Phys.* **160**, 164111 (2024).
- [47] See Supplemental Material for additional details.
- [48] T. Dornheim, “Fermion sign problem in path integral Monte Carlo simulations: Quantum dots, ultracold atoms, and warm dense matter,” *Phys. Rev. E* **100**, 023307 (2019).
- [49] Michael Bonitz, Jan Vorberger, Mandy Bethkenhagen, Maximilian Böhme, David Ceperley, Alexey Filinov, Thomas Gawne, Frank Graziani, Gianluca Gregori, Paul Hamann, Stephanie Hansen, Markus Holzmann, S. X. Hu, Hanno Köhlert, Valentin Karasiev, Uwe Kleinschmidt, Linda Kordts, Christopher Makait, Burkhard Militzer, Zhandos Moldabekov, Carlo Pierleoni, Martin Preising, Kushal Ramakrishna, Ronald Redmer, Sebastian Schwalbe, Pontus Svensson, and Tobias Dornheim, “First principles simulations of dense hydrogen,” (2024), [arXiv:2405.10627](https://arxiv.org/abs/2405.10627).
- [50] Thomas Gawne, Zhandos A. Moldabekov, Oliver S. Humphries, Karen Appel, Carsten Baetz, Victorien Bouffetier, Erik Brambrink, Attila Cangi, Sebastian Göde, Zuzana Konôpková, Mikako Makita, Mikhail Mishchenko, Motoaki Nakatsutsumi, Kushal Ramakrishna, Lisa Randolph, Sebastian Schwalbe, Jan Vorberger, Lennart Wollenweber, Ulf Zastra, Tobias Dornheim, and Thomas R. Preston, “Ultrahigh resolution x-ray thomson scattering measurements at the european x-ray free electron laser,” *Phys. Rev. B* **109**, L241112 (2024).